

Probing $B^+ \rightarrow K^+$ semi-leptonic FCNC decay with new physics effects under PQCD approach

Chao-Qi Zhang^{1,*}, Jin Sun^{2,†}, Zhi-Peng Xing^{1,‡} and Rui-Lin Zhu^{1§}

¹*Department of Physics and Institute of Theoretical Physics,*

Nanjing Normal University, Nanjing 210023, Jiangsu, China

²*Particle Theory and Cosmology Group, Center for Theoretical Physics of the Universe,
Institute for Basic Science (IBS), Daejeon 34126, Korea*

(Dated: January 3, 2025)

Recently, the Belle II Collaboration reported the branching fraction $\mathcal{B}(B^+ \rightarrow K^+ \nu \bar{\nu}) = (2.3 \pm 0.7) \times 10^{-5}$ with a significance of 3.5σ , which is 2.7σ above the SM expectation. Motivated by this measurement, we calculate this decay channel at the NLO and twist-3 level using the PQCD approach. By combining the lattice QCD data and our results, we obtain form factors with improved accuracy. Using these form factors, we precisely estimate the branching ratios of $B^+ \rightarrow K^+$ semileptonic FCNC decays, including $B^+ \rightarrow K^+ \nu \bar{\nu}$ and $B^+ \rightarrow K^+ \ell^+ \ell^-$. To explain the anomalies in these two processes, we introduce a leptoquark model as a new physics scenario. Using five possible types of leptoquarks, we successfully explain the latest experimental measurements, and further constraints on the leptoquarks are derived.

I. INTRODUCTION

The exclusive B decay processes play an extraordinarily important role in exploring the intricate dynamics of quark and lepton sectors, not only for precisely testing the Standard Model (SM) but also for searching for New Physics (NP) effects. Over the past 60 years, many important B decay processes have been measured in various experimental facilities and have been confirmed by SM predictions. With the accumulation of more and more experimental data [1–8], B decay physics is undoubtedly at the forefront of precisely testing the SM and searching for NP.

In B decay processes, semileptonic decays, which consist of a hadron and a lepton pair in the final state, are a focal point of research. Since the lepton pair and hadron in the final state hardly interact with each other, this reduces the uncertainties in theoretical studies. The decay amplitude is entirely determined by the hadronic matrix element, which can be expressed in terms of form factors. Among these, flavor-changing neutral current (FCNC) processes, in which prominent flavor anomalies have been observed, provide an ideal platform for precisely testing the SM and searching for NP. The FCNC processes are suppressed by the Glashow-Iliopoulos-Maiani (GIM) mechanism and are forbidden at tree level in the SM. The suppressed contribution from the SM makes these processes highly sensitive to NP effects. Recently, with the increase in experimental luminosity, the Belle II Collaboration has reported the first evidence for $B^+ \rightarrow K^+ \nu \bar{\nu}$ decay with a significance of 3.5 standard deviations as [9]

$$\mathcal{Br}(B^+ \rightarrow K^+ \nu \bar{\nu}) = (2.3 \pm 0.7) \times 10^{-5}. \quad (1)$$

The latest experimental progress has greatly stimulated interest in theoretical research [10–43].

Over the past decade, B decays have been extensively studied within the frameworks of perturbative QCD (PQCD) [44–58], lattice QCD (LQCD) [59–68], and QCD sum rules (QCDSR) [69–74]. The PQCD approach, as a method for perturbative QCD analysis, serves as a robust tool for estimating the matrix elements of semileptonic decays of B mesons in the low momentum transfer region [75–77]. It has demonstrated significant predictive power concerning B decays, particularly regarding CP violation [78–82]. Regarding the FCNC process $B^+ \rightarrow K^+$, LQCD has achieved the most precise determination of the $B \rightarrow K$ form factor [83], consistent with earlier PQCD calculations that included twist-2 and next-to-leading order (NLO) corrections [84]. Nevertheless, using this highly accurate form factor, the theoretical prediction for the branching ratio of $B^+ \rightarrow K^+ \nu \bar{\nu}$ differs from the experimental measurement by approximately 2.7 standard deviations [9] as

$$\frac{\mathcal{Br}(B^+ \rightarrow K^+ \nu \bar{\nu})_{th}}{\mathcal{Br}(B^+ \rightarrow K^+ \nu \bar{\nu})_{exp}} = 4.1 \pm 1.3. \quad (2)$$

The significant discrepancy between the theoretical predictions and experimental measurements necessitates considering higher-twist (twist-3) and higher-order (NLO) contributions within the PQCD framework, as well as potential NP effects in this process.

Among various NP models, leptoquarks (LQs) can introduce direct couplings between leptons and quarks [85, 86], thus bridging this fundamental connection between quark and lepton families. At low energies, leptoquarks can induce two-lepton-two-quark interactions similar to those mediated by electroweak four-fermion vertices, making them a promising framework for explaining the previously mentioned discrepancies. Leptoquarks, as new color-triplet particles that can manifest as either scalar or vector bosons and carry both lepton and baryon numbers, have been extensively utilized to explain a range of

* E-mail: cqzhang@nnu.edu.cn

† E-mail: sunjin0810@ibs.re.kr

‡ E-mail: zpxing@nnu.edu.cn

§ E-mail: rlzhu@njnu.edu.cn

experimental flavor anomalies [87–91]. These anomalies include $R_{K(*)}$, $R_{D(*)}$ and the muon's anomalous magnetic moment $(g-2)_\mu$ in scenarios where the LQ-lepton-quark couplings are not confined to a single generation. Additionally, searches for relevant collider signals have been conducted using various approaches [92, 93]. LQs typically decay into either a charged lepton and a quark or a neutrino and a quark. At conventional particle-antiparticle colliders, LQs can be produced in pairs, setting a lower limit on their mass to approximately half the center-of-mass energy of the accelerator. However, heavier LQs can only participate in t-channel exchanges, resulting in a smaller cross section for the interactions they mediate. For instance, at the LHC, the leading-order (LO) processes for leptoquark pair production primarily involve gluon-gluon fusion and quark-antiquark annihilation.

For the processes we have investigated, the flavor-changing neutral current $b \rightarrow s$ decays can occur via the exchange of a leptoquark as an intermediate state. In SM calculations, the uncertainties in our predictions can be significantly reduced by integrating LQCD data from high-momentum-transfer regions with PQCD calculations at low momentum transfers. The improved precision of SM predictions, coupled with the significant discrepancy between experimental results and theoretical expectations, underscores the necessity for deeper exploration into the constraints on leptoquark parameters, such as their masses and couplings, within our study.

This paper is organized as follows: In Section II, we define the kinematics of the decay and give the necessary inputs for our calculations. In Section III, we write down the observables of the process and present our numerical results and discussion in SM. In Section V, we introduce the LQ model and place constraints on the NP parameters. In Section VI, we make a brief summary. Some useful expressions are listed in the Appendix A.

II. KINEMATICS AND WAVE FUNCTIONS

In our work, the theoretical calculation are given under the PQCD factorization framework. In the rest frame of B meson, the momentum of B and K can be defined as

$$p_1 = \frac{M_B}{\sqrt{2}} (1, 1, \mathbf{0}_T), \quad p_2 = \frac{M_B}{\sqrt{2}} (0, \eta, \mathbf{0}_T), \quad (3)$$

under the light-cone coordinates, respectively. M_B is the mass of B meson, η is the energy fraction carried by K . Here we define the transfer momentum $q = p_1 - p_2$, then the energy fraction $\eta = 1 - q^2/M_B^2$. The momenta of light quarks in the B and K shown in Fig. 1 are written as

$$k_1 = \frac{M_B}{\sqrt{2}} (x_1, 0, \mathbf{k}_{1T}), \quad k_2 = \frac{M_B}{\sqrt{2}} (0, \eta x_2, \mathbf{k}_{2T}), \quad (4)$$

where x_1 and x_2 are parton momentum fractions. \mathbf{k}_{1T} and \mathbf{k}_{2T} are the transverse momentum. In this factorization approach, the scales which are involved in this

processes can be divided as $m_b^2 \gg m_b \Lambda_{\text{QCD}} \gg \Lambda_{\text{QCD}}^2$. The part with scale m_b^2 and $m_b \Lambda_{\text{QCD}}$ can be perturbative calculated called hard scattering kernel and the left part are factorized as non-perturbative input called wave function. This type of factorization may suffer endpoint singularities [94–96]. A notable feature of PQCD is the preservation of transverse momentum k_T to eliminate end-point divergences [97]. In this strategy, the decay amplitude can be factorized into the convolution of the wilson coefficient C , hard scattering kernel H , the hadronic wave functions ϕ , jet function J_t and Sudakov factor S as

$$\mathcal{A} = C \otimes H \otimes \phi \otimes J_t \otimes S. \quad (5)$$

Here the jet function and Sudakov factor comes from the k_T resummation and threshold resummation respectively [98]. The hadronic wave function which are expressed by the Light-Cone-Distribution-Amplitude (LCDAs) can be extracted from experiments or other non-perturbative methods [99–104].

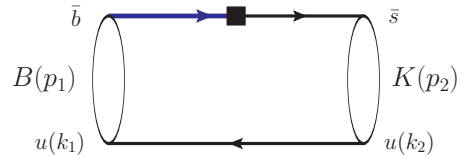


FIG. 1: The Feynman diagrams for $B \rightarrow K$ transition which include the momenta of quark in initial and final meson states. The black block represent vertices for weak interactions. The gluon propagator are omitted in this figure.

The B meson DA is defined via the matrix element as

$$\int \frac{d^4 z}{(2\pi)^4} e^{ik \cdot z} \langle 0 | b_\alpha(0) \bar{q}_\beta(z) | \bar{B}(p_1) \rangle = \frac{i}{\sqrt{2N_c}} \left((\not{p}_1 + M_B) \gamma_5 \left[\phi_B(k) - \frac{\not{p} - \not{k}}{\sqrt{2}} \bar{\phi}_B(k) \right] \right)_{\alpha\beta} \quad (6)$$

where $n = (1, 0, \mathbf{0}_T)$ and $\bar{n} = (0, 1, \mathbf{0}_T)$. $N_c = 3$ is the number of colors. For the distribution amplitudes(DAs), we adopt [77]

$$\phi_B(x, b) = N_B x^2 (1-x)^2 \exp \left[-\frac{x^2 M_B^2}{2\omega_b^2} - \frac{\omega_b^2 b^2}{2} \right], \quad (7)$$

where $\omega_b = 0.40 \pm 0.04$ is shape parameter and b is the parameter conjugate to \mathbf{k}_T . The normalization constant N_B satisfied

$$\int_0^1 \phi_B(x, b=0) dx = \frac{f_B}{2\sqrt{2N_c}}, \quad (8)$$

with decay constant f_B . The light meson LCDAs are also defined through the matrix elements as

$$\begin{aligned} \langle K(p_2) | q_{1\alpha}(0) \bar{q}_{2\beta}(z) | 0 \rangle &= \frac{i}{\sqrt{2N_c}} \int_0^1 dx e^{ixp \cdot z} \\ &\times [\gamma_5 \not{p}_2 \phi_K^A(x) + \gamma_5 m_0^K \phi_K^P(x) + m_0^K \gamma_5 (\not{p} - \not{k}) \phi_K^T(x)] \end{aligned} \quad (9)$$

where the wave function of K meson is given by

$$\Phi_K(x) = \frac{i}{\sqrt{2N_c}} \times \gamma_5 [\not{p}_2 \phi_K^A(x) + m_0^K \phi_K^P(x) - m_0^K (\not{p} \not{h} - 1) \phi_K^T(x)] \quad (10)$$

where $m_0^K = 1.6$ GeV is chiral mass of the K meson. The kaon meson DAs up to twist-3 are

$$\begin{aligned} \phi_K^A(x) &= \frac{f_K}{2\sqrt{6}} 6x(1-x) \left[1 + a_1^K C_1^{3/2}(t) + a_2^K C_2^{3/2}(t) + a_4^K C_4^{3/2}(t) \right], \\ \phi_K^P(x) &= \frac{f_K}{2\sqrt{6}} \left[1 + \left(30\eta_3 - \frac{5}{2}\rho_K^2 \right) C_2^{1/2}(t) - 3 \left(\eta_3\omega_3 + \frac{9}{20}\rho_K^2 (1+6a_2^K) \right) C_4^{1/2}(t) \right], \\ \phi_K^T(x) &= \frac{f_K}{2\sqrt{6}} (1-2x) \left[1 + 6 \left(5\eta_3 - \frac{1}{2}\eta_3\omega_3 - \frac{7}{20}\rho_K^2 - \frac{3}{5}\rho_K^2 a_2^K \right) (1-10x+10x^2) \right], \end{aligned} \quad (11)$$

with $\rho_K = M_K/m_0^K$, M_K and f_K are the mass and decay constant of K meson, respectively. The Gegenbauer polynomials are [99, 100]

$$\begin{aligned} C_1^{3/2}(t) &= 3t, \quad C_2^{1/2}(t) = \frac{1}{2}(3t^2 - 1), \\ C_2^{3/2}(t) &= \frac{3}{2}(5t^2 - 1), \\ C_4^{1/2}(t) &= \frac{1}{8}(3 - 30t^2 + 35t^4), \\ C_4^{3/2}(t) &= \frac{15}{8}(1 - 14t^2 + 21t^4), \end{aligned} \quad (12)$$

with $t = 2x - 1$, the Gegenbauer moments are [99, 100]

$$\begin{aligned} a_1^K &= 0.06, \quad a_2^K = 0.25 \pm 0.15, \quad a_4^K = -0.015, \\ \eta_3^K &= 0.015, \quad \omega_3^K = -3.0. \end{aligned} \quad (13)$$

III. THEORETICAL CALCULATIONS

Utilizing the provided LCDAs, we can analytically compute the semi-leptonic FCNC decay process of $B^+ \rightarrow K^+$. The considered Feynman diagrams are illustrated in Fig. 2. This figure depicts both the short-distance (SD) interactions, as represented by the low-energy effective Hamiltonian, and the long-distance (LD) interactions.

The low energy effective Hamiltonian of $b \rightarrow s\nu\bar{\nu}$ transitions can be written as [105]

$$\mathcal{H}_{\text{eff}} = -\frac{4G_F}{\sqrt{2}} \frac{\alpha_{em}}{2\pi} V_{tb} V_{ts}^* C_{\text{SM}}^{LL} \mathcal{O}_V^{LL}, \quad (14)$$

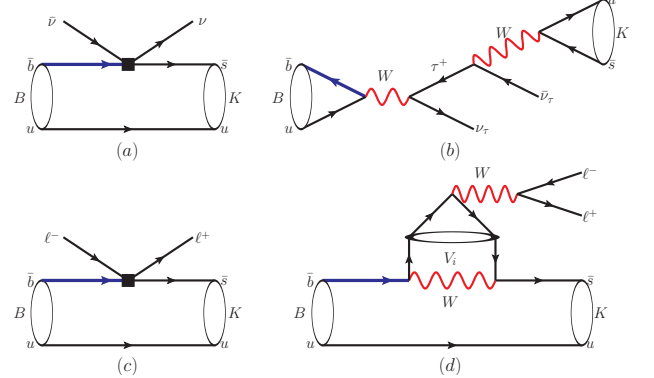


FIG. 2: The Feynman diagrams for $B \rightarrow K$ FCNC processes. The figure in first line show the diagram of $B^+ \rightarrow K^+ \nu \bar{\nu}$ including SD(left) and LD(right) contribution. The second line figures are the diagram of $B^+ \rightarrow K^+ \ell^+ \ell^-$ including SD(left) and LD(right) contribution.

where G_F is the Fermi coupling constant, α_{em} is the coupling constant of electromagnetic interaction, V_{ij} is the CKM matrix elements, C is the Wilson coefficients. The four-fermion operator is

$$\mathcal{O}_V^{LL} = (\bar{s}\gamma^\mu P_L b)(\bar{\nu}\gamma_\mu P_L \nu), \quad (15)$$

with

$$C_{\text{SM}}^{LL} = -X_t / \sin^2(\theta_W) = -6.32(7). \quad (16)$$

Here $X_t = 1.462(17)$. It includes the next-to-leading order (NLO) Quantum Chromodynamics (QCD) corrections and the two-loop electroweak contributions.

For $b \rightarrow s\ell^+\ell^-$ processes, the low energy effective Hamiltonian is

$$\begin{aligned} \mathcal{H}_{\text{eff}} = -\frac{4G_F}{\sqrt{2}} V_{tb} V_{ts}^* &\left\{ \left[C_1(\mu) \mathcal{O}_1^c(\mu) + C_2(\mu) \mathcal{O}_2^c(\mu) \right. \right. \\ &+ \sum_{i=3}^{10} C_i(\mu) \mathcal{O}_i(\mu) \Big] + \lambda_u \left[C_1(\mu) (\mathcal{O}_1^c(\mu) \right. \\ &\left. \left. - \mathcal{O}_1^u(\mu)) + C_2(\mu) (\mathcal{O}_2^c(\mu) - \mathcal{O}_2^u(\mu)) \right] \right\}, \end{aligned} \quad (17)$$

where $\lambda_u = V_{ub} V_{us}^* / (V_{tb} V_{ts}^*)$. $C_i(\mu)$ are Wilson coefficients, $\mathcal{O}_i(\mu)$ are four fermion operators, they all depend on the renormalization scale μ . For notational simplicity,

we will omit the symbol μ in the subsequent discussion.

$$\begin{aligned}
\mathcal{O}_1^c &= (\bar{s}_\alpha \gamma^\mu P_L c_\beta)(\bar{c}_\beta \gamma_\mu P_L b_\alpha), \\
\mathcal{O}_2^c &= (\bar{s}_\alpha \gamma^\mu P_L c_\alpha)(\bar{c}_\beta \gamma_\mu P_L b_\beta), \\
\mathcal{O}_1^u &= (\bar{s}_\alpha \gamma^\mu P_L u_\beta)(\bar{u}_\beta \gamma_\mu P_L b_\alpha), \\
\mathcal{O}_2^u &= (\bar{s}_\alpha \gamma^\mu P_L u_\alpha)(\bar{u}_\beta \gamma_\mu P_L b_\beta), \\
\mathcal{O}_3 &= (\bar{s}_\alpha \gamma^\mu P_L b_\alpha) \sum_q (\bar{q}_\beta \gamma_\mu P_L q_\beta), \\
\mathcal{O}_4 &= (\bar{s}_\alpha \gamma^\mu P_L b_\beta) \sum_q (\bar{q}_\beta \gamma_\mu P_L q_\alpha), \\
\mathcal{O}_5 &= (\bar{s}_\alpha \gamma^\mu P_L b_\alpha) \sum_q (\bar{q}_\beta \gamma_\mu P_L q_\beta), \\
\mathcal{O}_6 &= (\bar{s}_\alpha \gamma^\mu P_L b_\beta) \sum_q (\bar{q}_\beta \gamma_\mu P_L q_\alpha), \\
\mathcal{O}_7 &= \frac{em_b}{16\pi^2} \bar{s} \sigma^{\mu\nu} P_R b F_{\mu\nu}, \\
\mathcal{O}_8 &= \frac{gm_b}{16\pi^2} \bar{s} \sigma^{\mu\nu} T^a P_R b G_{\mu\nu}^a, \\
\mathcal{O}_9 &= \frac{\alpha_{em}}{4\pi} (\bar{s} \gamma^\mu P_L b) (\bar{\ell} \gamma_\mu \ell), \\
\mathcal{O}_{10} &= \frac{\alpha_{em}}{4\pi} (\bar{s} \gamma^\mu P_L b) (\bar{\ell} \gamma_\mu \gamma_5 \ell),
\end{aligned} \tag{18}$$

$F_{\mu\nu}$ and $G_{\mu\nu}^a$ are the electromagnetic and chromomagnetic tensors, respectively. T^a is the generators of the $SU(3)_C$ group.

Based on the effective Hamiltonian, the transition amplitude for the $B \rightarrow K$ flavor-changing neutral current (FCNC) process comprises both hadronic and leptonic matrix elements. The hadronic matrix element can be parameterized by the form factors $F_+(q^2)$, $F_0(q^2)$ and $F_T(q^2)$ as

$$\begin{aligned}
\langle K(p_2) | \bar{s}(0) \gamma_\mu b(0) | B(p_1) \rangle &= \left[\frac{M_B^2 - M_K^2}{q^2} q_\mu \right] F_0(q^2) \\
&\quad + \left[(p_1 + p_2)_\mu - \frac{M_B^2 - M_K^2}{q^2} q_\mu \right] F_+(q^2), \\
\langle K(p_2) | \bar{s}(0) \sigma_{\mu\nu} b(0) | B(p_1) \rangle &= \frac{2i[p_{2\mu} q_\nu - q_\mu p_{2\nu}]}{M_B + M_K} F_T(q^2).
\end{aligned} \tag{19}$$

It is straightforward to observe that setting $q^2 = 0$, $F_+(0)$ results in $F_0(0)$.

For B decay processes, leading-order (LO) calculations are insufficiently precise for testing the Standard Model (SM). Next-to-leading-order (NLO) corrections have been extensively considered in semi-leptonic B decays. The NLO $B \rightarrow \pi$ transition form factors at twist-2 are provided in Ref. [106]. Utilizing these results, the form factors for $B \rightarrow K$, $B_s \rightarrow K$, and $B \rightarrow \pi$ transitions were calculated in Ref. [84]. These NLO contributions amount to approximately 20%. In addition to higher-order corrections, higher-twist effects have also been evaluated in recent studies. The NLO twist-3 contributions to $B \rightarrow \pi$ transition form factors have been considered in Ref. [107]. It was found that the NLO

twist-3 and twist-2 contributions are of similar magnitude but opposite sign, resulting in significant cancellation between them [107]. Consequently, the NLO twist-3 contribution must be accounted for in this study. Given that the behavior of $B \rightarrow K$ processes is analogous to that of $B \rightarrow \pi$ transitions, by following the methodology outlined in Refs. [106, 107], we can readily recalculate the $B \rightarrow K$ form factors at NLO. The NLO PQCD factorization formulas for $F_0(q^2)$, $F_+(q^2)$, and $F_T(q^2)$ are

$$\begin{aligned}
F_0(q^2)|_{\text{NLO}} &= 8\pi C_f M_B^2 \int dx_1 dx_2 \int b_1 db_1 b_2 db_2 \\
&\quad \times \phi_B(x_1, b_1) \{ (2 - \eta) r_K [\phi_K^P(x_2) - \phi_K^T(x_2)] \\
&\quad \times \alpha_s(t_1) h(x_1, x_2, b_1, b_2) e^{-S_{BK}(t_1)} S_t(x_2) \\
&\quad + \eta [(1 + x_2 \eta) (1 + F_{T2}^{(1)}(x_i, \mu, t, q^2)) \phi_K^A(x_2) \\
&\quad - 2r_K x_2 \phi_K^P(x_2) + 2r_K (1/\eta - x_2) \phi_K^T(x_2)] \\
&\quad \times \alpha_s(t_1) h(x_1, x_2, b_1, b_2) e^{-S_{BK}(t_1)} S_t(x_2) \\
&\quad + \eta [2r_K (1 + F_{T3}^{(1)}(x_i, \mu, t, q^2)) \phi_K^P(x_2)] \alpha_s(t_2) \\
&\quad \times h(x_2, x_1, b_2, b_1) e^{-S_{BK}(t_2)} S_t(x_1) \}, \\
F_+(q^2)|_{\text{NLO}} &= 8\pi C_f M_B^2 \int dx_1 dx_2 \int b_1 db_1 b_2 db_2 \\
&\quad \times \phi_B(x_1, b_1) \{ r_K [\phi_K^P(x_2) - \phi_K^T(x_2)] \\
&\quad \times \alpha_s(t_1) h(x_1, x_2, b_1, b_2) e^{-S_{BK}(t_1)} S_t(x_2) \\
&\quad + [(1 + x_2 \eta) (1 + F_{T2}^{(1)}(x_i, \mu, t, q^2)) \phi_K^A(x_2) \\
&\quad - 2r_K x_2 \phi_K^P(x_2) + 2r_K (1/\eta - x_2) \phi_K^T(x_2)] \\
&\quad \times \alpha_s(t_1) h(x_1, x_2, b_1, b_2) e^{-S_{BK}(t_1)} S_t(x_2) \\
&\quad + [2r_K (1 + F_{T3}^{(1)}(x_i, \mu, t, q^2)) \phi_K^P(x_2)] \alpha_s(t_2) \\
&\quad \times h(x_2, x_1, b_2, b_1) e^{-S_{BK}(t_2)} S_t(x_1) \}, \\
F_T(q^2)|_{\text{NLO}} &= 8\pi C_f M_B^2 (1+r) \int dx_1 dx_2 \int b_1 db_1 b_2 db_2 \\
&\quad \times \phi_B(x_1, b_1) \{ [(1 + F_{T2}^{(1)}(x_i, \mu, t, q^2)) \phi_K^A(x_2) \\
&\quad - r_K x_2 \phi_K^P(x_2) + r_K (2/\eta + x_2) \phi_K^T(x_2)] \\
&\quad \times \alpha_s(t_1) h(x_1, x_2, b_1, b_2) e^{-S_{BK}(t_1)} S_t(x_2) \\
&\quad + [2r_K (1 + F_{T3}^{(1)}(x_i, \mu, t, q^2)) \phi_K^P(x_2)] \alpha_s(t_2) \\
&\quad \times h(x_2, x_1, b_2, b_1) e^{-S_{BK}(t_2)} S_t(x_1) \},
\end{aligned} \tag{20}$$

with color factor $C_f = 4/3$, $r = M_K/M_B$, $r_K = m_0^K/M_B$. In this context, we have omitted the terms proportional to x_1 , as they are power-suppressed. The running coupling constant α_s , hard function h , Sudakov exponent S_{BK} , and threshold resummation factor S_t can be found in the Appendix A. NLO hard kernel $F_{T2}^{(1)}(x_i, \mu, t, q^2)$ and $F_{T3}^{(1)}(x_i, \mu, t, q^2)$ are also listed in Appendix A.

IV. NUMERICAL RESULTS

After constructing the factorization formula for the form factors, we can compute the required form factors

using the provided input parameters. The input parameters used in our calculations are summarized as follows. The masses are taken as (in units of GeV) [8]

$$\begin{aligned} M_B &= 5.280, & M_K &= 0.494, \\ m_\tau &= 1.777, & m_W &= 80.42, \\ m_t &= 172.57, & m_b &= 4.209, & m_c &= 1.272. \end{aligned} \quad (21)$$

The lifetime (in units of ps) and decay constant (in units of GeV) are [8]

$$\tau_B = 1.638, \quad f_B = 0.21, \quad f_K = 0.16. \quad (22)$$

For the CKM matrix elements, we adopt [8]

$$\begin{aligned} |V_{ub}| &= (3.82 \pm 0.20) \times 10^{-3}, & |V_{us}| &= 0.22431 \pm 0.00085, \\ |V_{tb}| &= 1.010 \pm 0.027, & |V_{ts}| &= (41.5 \pm 0.9) \times 10^{-3}. \end{aligned} \quad (23)$$

Wilson Coefficients at $\mu = m_b$ [108]

$$\begin{aligned} C_1 &= -0.294(9), & C_2 &= 1.017(1), & C_3 &= -0.0059(2), \\ C_4 &= -0.087(1), & C_5 &= 0.0004, & C_6 &= 0.0011(1), \\ C_7 &= -0.2957(5), & C_8 &= -0.1630(6), & C_9 &= 4.114(14), \\ C_{10} &= -4.193(33). \end{aligned} \quad (24)$$

Other parameters [8]

$$\begin{aligned} G_F &= 1.1663788(6) \times 10^{-5} \text{ GeV}^{-2}, \\ 1/\alpha_{em}(M_Z) &= 127.952(9), \quad \gamma = 0.5772156649. \end{aligned} \quad (25)$$

A. Form factors

Using the input parameters and factorization formula presented above, we can estimate the numerical results for the form factors, which are summarized in Tables I and II. In Table I, we detail the contributions from each order and twist. It can be observed that the NLO twist-2 and twist-3 contributions are approximately equal in magnitude but have opposite signs, leading to an overall enhancement of only about $3\% \sim 4\%$ relative to the full LO contribution. This finding aligns with the conclusions drawn in Ref. [107]. In Table II, we compare our results with those from other theoretical studies. The results show consistency among each other within the uncertainties. Within the PQCD framework, the primary sources of uncertainty stem from the shape parameter ω_B in the B meson distribution amplitudes (DAs) and the Gegenbauer moments of the final-state meson wave functions. Taking into account the uncertainties associated with the input parameters, the total error in our calculations is approximately 20%.

While PQCD offers reliable predictions, it is particularly effective for calculations in the low- q^2 region. Conversely, LQCD provides more precise results in the high- q^2 region. Hence, we follow the approach outlined in Ref. [54], employing PQCD for the low- q^2 region and integrating LQCD results for the high- q^2 region to model

TABLE I: Central values of $B \rightarrow K$ transition form factors at $q^2 = 0$, the label LO, LO+NLO(T-2), LO+NLO(T-3), and LO+NLO mean the full LO contribution, the full LO plus NLO twist-2 contribution, the full LO plus NLO twist-3 contribution, and the total contribution of LO and NLO, respectively.

	LO	LO+NLO(T-2)	LO+NLO(T-3)	LO+NLO
$F_0(0)$	0.326	0.381(+17%)	0.284(-13%)	0.340(+4%)
$F_+(0)$	0.326	0.381(+17%)	0.284(-13%)	0.340(+4%)
$F_T(0)$	0.345	0.399(+16%)	0.299(-13%)	0.354(+3%)

the form factors over the full kinematic range. The q^2 dependence of the form factors is described using the BCL parametrization [112]

$$z(q^2) = \frac{\sqrt{t_+ - q^2} - \sqrt{t_+ - t_0}}{\sqrt{t_+ - q^2} + \sqrt{t_+ - t_0}}, \quad (26)$$

with $t_+ = (M_B + M_K)^2$, $t_0 = t_+(1 - \sqrt{1 - t_-/t_+})$, then the form factor can be expressed as

$$\begin{aligned} f_0(q^2) &= \frac{\mathcal{L}}{1 - \frac{q^2}{M_{R0}^2}} \sum_{n=0}^{N-1} \alpha_n^0 z^n \\ f_+(q^2) &= \frac{\mathcal{L}}{1 - \frac{q^2}{M_{R+}^2}} \sum_{n=0}^{N-1} \alpha_n^+ \left(z^n - \frac{n}{N} (-1)^{n-N} z^N \right) \\ f_T(q^2) &= \frac{\mathcal{L}}{1 - \frac{q^2}{M_{RT}^2}} \sum_{n=0}^{N-1} \alpha_n^T \left(z^n - \frac{n}{N} (-1)^{n-N} z^N \right). \end{aligned} \quad (27)$$

with $\mathcal{L} = 1.304$, $M_{R0} = 5.729$ GeV, $M_{R+,RT} = 5.416$ GeV [83].

The parameters α_n^i , listed in Table III, are obtained from the fitting process. Using these fitted parameters, we illustrate the q^2 -dependence of the form factors in Fig. 3.. Leveraging LQCD data, we are able to further reduce uncertainties in the high- q^2 region. It should be noted that the calculation range for the previous PQCD approach was $0 \leq q^2 \leq 12$ GeV 2 . According to Ref. [54], it is recommended to narrow this range to $0 \leq q^2 \leq m_\tau^2$. Consequently, we have adopted the range $0 \leq q^2 \leq 3$ GeV 2 .

B. $B^+ \rightarrow K^+ \nu \bar{\nu}$

Based on the form factors we have fitted, we can give the decay branching ratios as

$$\begin{aligned} \mathcal{B}(B^+ \rightarrow K^+ \nu \bar{\nu})|_{\text{SD}} &= \tau_{B^+} \int dq^2 \frac{3G_F^2 \alpha_{em}^2 \lambda_K^{3/2}}{768\pi^5 M_B^3} |V_{tb} V_{ts}^*|^2 |C_{\text{SM}}^{LL}|^2 |F_+(q^2)|^2, \\ (28) \end{aligned}$$

TABLE II: Results of $B \rightarrow K$ transition form factors at $q^2 = 0$ obtained by using different theories. Results of $B^+ \rightarrow K^+ \ell \bar{\ell}$ branching ratios obtained by using different theories. The data in the fourth, sixth, and seventh column includes both SD and LD contributions, while the other data includes only SD contributions. The errors in our results originate from form factors. We added the errors mentioned in the references in quadrature. SD results of $B^+ \rightarrow K^+ \nu \bar{\nu}$ branching ratios (10^{-6}) for various q^2 bins obtained by using different theories.

	PQCD(previous)[84]	QCDSR[10, 99, 109]	LQCD[83, 110]	SCET[111]	This work	Data
$F_0(0)$	0.310 ± 0.054	0.331 ± 0.041	0.332 ± 0.012	0.325 ± 0.085	0.340 ± 0.059	...
$F_+(0)$	0.310 ± 0.054	0.331 ± 0.041	0.332 ± 0.012	0.325 ± 0.085	0.340 ± 0.059	...
$F_T(0)$	0.340 ± 0.062	0.358 ± 0.037	0.332 ± 0.024	0.351 ± 0.097	0.354 ± 0.066	...
$\mathcal{B}(B^+ \rightarrow K^+ \nu \bar{\nu})(10^{-6})$	$4.42^{+1.66}_{-1.36}$	$4.135^{+0.820}_{-0.655}$	5.67 ± 0.38	$5.239^{+0.311}_{-0.281}$	5.70 ± 0.17	23 ± 7
$\mathcal{B}(B^+ \rightarrow K^+ \ell^+ \ell^-)(10^{-7})$	$5.50^{+2.06}_{-1.69}$	$6.633^{+1.341}_{-1.070}$	7.04 ± 0.55	...	7.21 ± 0.23	4.7 ± 0.5
$q^2 \in (0, 4)$...	0.93 ± 0.15	1.189 ± 0.097	$1.282^{+0.087}_{-0.080}$	1.154 ± 0.059	...
$q^2 \in (4, 8)$...	0.92 ± 0.12	1.155 ± 0.090	$1.224^{+0.076}_{-0.069}$	1.117 ± 0.036	...
$q^2 \in (8, 12)$...	0.86 ± 0.10	1.071 ± 0.084	$1.112^{+0.066}_{-0.060}$	1.032 ± 0.021	...
$q^2 \in (12, 16)$...	0.71 ± 0.08	0.905 ± 0.072	$0.916^{+0.053}_{-0.048}$	0.869 ± 0.015	...
$q^2 \in (16, 20)$...	0.55 ± 0.06	0.597 ± 0.048	$0.705^{+0.040}_{-0.036}$	0.571 ± 0.013	...
$q^2 \in (20, q_{max}^2)$...		0.127 ± 0.011		0.122 ± 0.004	...

TABLE III: The fitted out parameters by BCL parametrization.

Form factor(fit)	α_0	α_1	α_2
$F_+(0)$	0.335 ± 0.010	$0.257(8)$	$-0.703(88)$
$F_0(0)$	0.333 ± 0.008	$0.256(6)$	$0.216(44)$
$F_T(0)$	0.346 ± 0.017	$0.266(13)$	$-0.62(14)$

where $\lambda_K = \lambda(M_B^2, M_K^2, q^2)$ is the Källén function as

$$\lambda(a, b, c) = a^2 + b^2 + c^2 - 2ab - 2bc - 2ac. \quad (29)$$

The SD contribution is $4.86(15) \times 10^{-6}$. For comparing with the experimental data, we also calculate the LD contribution [113]

$$\begin{aligned} \mathcal{B}(B^+ \rightarrow K^+ \nu \tau \bar{\nu}_\tau)|_{LD} &= \tau_{B^+} \frac{|G_F^2 V_{ub} V_{us}^* f_{K^+} f_{B^+}|^2}{256 \pi^3 M_{B^+}^3} \\ &\times \tau_\tau 2\pi m_\tau (M_{B^+}^2 - m_\tau^2)^2 (M_{K^+}^2 - m_\tau^2)^2, \end{aligned} \quad (30)$$

the contribution of LD interaction is $8.41(88) \times 10^{-7}$ which could account for 15% of the total $B^+ \rightarrow K^+ \nu \bar{\nu}$ rates, but it doesn't seem to be enough to explain the deviation between theory and experiment. Our numerical results, along with other theoretical predictions, are summarized in Table II. Overall, our results are consistent with those from various theoretical approaches, yet they are notably lower than the experimental data reported by Belle II. In Table II, we present the values for different q^2 bins for a more detailed comparison. Ad-

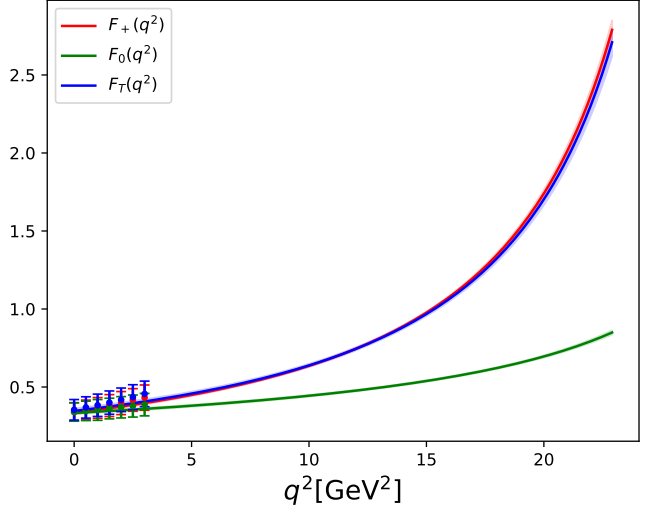


FIG. 3: The q^2 -dependence of the form factors in our fit.

ditionally, we illustrate the q^2 -dependence of the differential branching ratio in Fig. 4. It is evident that in the medium and high- q^2 regions, the uncertainties are relatively small. However, due to the somewhat larger uncertainties in our PQCD calculations, the confidence band in the low- q^2 region appears slightly broader.

For clear seeing the difference between experimental measurements and our results, we obtain

$$R_K^\nu \equiv \frac{\mathcal{B}(B \rightarrow K^+ \bar{\nu}\nu)}{\mathcal{B}(B \rightarrow K^+ \bar{\nu}\nu)|_{SM}} = 4.0 \pm 1.2, \quad (31)$$

This indicates that the experimental data are roughly

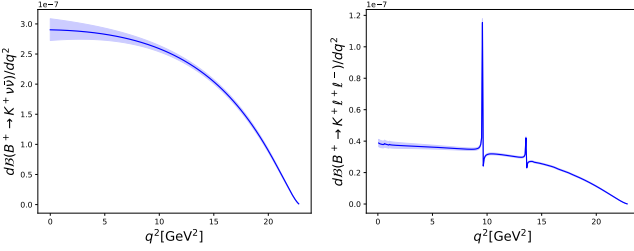


FIG. 4: The q^2 -dependence of the differential branching ratio.

four times higher than the theoretical predictions. To account for this significant discrepancy, one possibility is to introduce NP effects. Further analysis is provided in the following section.

C. $B^+ \rightarrow K^+ \ell^+ \ell^-$

As for the $B^+ \rightarrow K^+ \ell^+ \ell^-$ process, the contributions from $O_{1-6,8}$ which including SD and LD interaction can be added to the effective Wilson coefficients $O_{7,9}^{\text{eff}}$, then the effective Hamiltonian can be simplified to

$$\mathcal{H}_{\text{eff}} = -\frac{4G_F}{\sqrt{2}} V_{tb} V_{ts}^* \frac{\alpha_{em}}{4\pi} \left\{ C_{10} [\bar{s}\gamma^\mu P_L b][\bar{\ell}\gamma_\mu \gamma_5 \ell] + C_9^{\text{eff}} [\bar{s}\gamma^\mu P_L b][\bar{\ell}\gamma_\mu \ell] - 2m_b C_7^{\text{eff}} \left[\bar{s}i\sigma^{\mu\nu} \frac{q_\nu}{q^2} P_R b \right] [\bar{\ell}\gamma_\mu \ell] \right\}. \quad (32)$$

C_7^{eff} and C_9^{eff} are defined as

$$C_7^{\text{eff}} = C_7 + C'_{b \rightarrow s\gamma}, \quad C_9^{\text{eff}} = C_9 + Y_{\text{pert}}(\hat{s}) + Y_{\text{res}}(\hat{s}), \quad (33)$$

with $\hat{s} = q^2/M_B^2$. The term who contains the contributions of $b \rightarrow s\gamma$ is given by

$$C'_{b \rightarrow s\gamma} = i\alpha_s(m_b) \left\{ \frac{2}{9} \eta^{14/23} \left[\frac{x_t(x_t^2 - 5x_t - 2)}{8(x_t - 1)^3} + \frac{3x_t^2 \ln x_t}{4(x_t - 1)^4} - 0.1687 \right] - 0.03C_2 \right\}, \quad (34)$$

where $\eta = \alpha_s(m_W)/\alpha_s(\mu)$ and $x_t = m_t^2/m_W^2$. The term $Y_{\text{pert}}(\hat{s})$ contains the SD perturbative contributions

$$Y_{\text{pert}}(\hat{s}) = 0.124\omega(\hat{s}) + g(\hat{m}_c, \hat{s})C_0 + \lambda_u [g(\hat{m}_c, \hat{s}) - g(0, \hat{s})] (3C_1 + C_2) - \frac{1}{2}g(0, \hat{s})(C_3 + 3C_4) - \frac{1}{2}g(\hat{m}_b, \hat{s})(4C_3 + 4C_4 + 3C_5 + C_6) + \frac{2}{9}(3C_3 + C_4 + 3C_5 + C_6), \quad (35)$$

with $C_0 = 3C_1 + C_2 + 3C_3 + C_4 + 3C_5 + C_6$, $\hat{m}_q = m_q/m_b$. $\omega(\hat{s})$ can be defined as

$$\begin{aligned} \omega(\hat{s}) = & -\frac{2}{9}\pi^2 + \frac{4}{3} \int_0^{\hat{s}} \frac{\ln(1-u)}{u} du - \frac{2}{3} \ln(\hat{s}) \ln(1-\hat{s}) \\ & - \frac{5+4\hat{s}}{3(1+2\hat{s})} \ln(1-\hat{s}) - \frac{2\hat{s}(1+\hat{s})(1-2\hat{s})}{3(1-\hat{s})^2(1+2\hat{s})} \ln(\hat{s}) \\ & + \frac{5+9\hat{s}-6\hat{s}^2}{6(1-\hat{s})(1+2\hat{s})}. \end{aligned} \quad (36)$$

The functions $g(\hat{m}_q, \hat{s})$ and $g(0, \hat{s})$ are of the form

$$\begin{aligned} g(\hat{m}_q, \hat{s}) = & -\frac{8}{9} \ln(\hat{m}_q) + \frac{8}{27} + \frac{4}{9}x - \frac{2}{9}(2+x)\sqrt{|1-x|} \\ & \times \begin{cases} \ln \left| \frac{1+\sqrt{1-x}}{1-\sqrt{1-x}} \right| - i\pi, & x < 1, \\ 2 \arctan \frac{1}{\sqrt{x-1}}, & x > 1, \end{cases} \\ g(0, \hat{s}) = & \frac{8}{27} - \frac{8}{9} \ln \frac{m_b}{\mu} - \frac{4}{9} \ln \hat{s} + \frac{4}{9}i\pi, \end{aligned} \quad (37)$$

with $x = 4\hat{m}_q^2/\hat{s}$. The term $Y_{\text{res}}(\hat{s})$ refers to the LD contributions

$$\begin{aligned} Y_{\text{res}}(\hat{s}) = & -\frac{3\pi}{\alpha_{em}^2} \left[C_0 \sum_{V_i} \frac{M_{V_i} \mathcal{B}(V_i \rightarrow \ell^+ \ell^-) \Gamma_{V_i}}{q^2 - M_{V_i}^2 + iM_{V_i} \Gamma_{V_i}} \right. \\ & \left. - \lambda_u g(0, \hat{s})(3C_1 + C_2) \right. \\ & \left. \times \sum_{V_j} \frac{M_{V_j} \mathcal{B}(V_j \rightarrow \ell^+ \ell^-) \Gamma_{V_j}}{q^2 - M_{V_j}^2 + iM_{V_j} \Gamma_{V_j}} \right]. \end{aligned} \quad (38)$$

Light vector mesons and charmonium states which may contribute are listed in Table IV.

TABLE IV: Vector mesons masses, widths and branching ratios to $\ell^+ \ell^-$ [8].

V_i	M_{V_i} (GeV)	Γ_{V_i} (MeV)	$\mathcal{B}(V_i \rightarrow \ell^+ \ell^-)$
ρ	0.775	149	4.635×10^{-5}
ω	0.783	8.68	7.380×10^{-5}
ϕ	1.019	4.249	2.915×10^{-4}
J/ψ	3.097	0.093	5.966×10^{-2}
$\psi(2S)$	3.686	0.294	7.965×10^{-3}
$\psi(3770)$	3.774	27.2	9.6×10^{-6}
$\psi(4040)$	4.039	80	1.07×10^{-5}
$\psi(4160)$	4.191	70	6.9×10^{-6}

Then the branching ratios can be given by

$$\begin{aligned} \mathcal{B}(B^+ \rightarrow K^+ \ell^+ \ell^-) &= \tau_{B^+} \int dq^2 \frac{G_F^2 \alpha_{em}^2 |V_{tb}|^2 |V_{ts}^*|^2 \sqrt{\lambda(q^2)}}{512 M_B^3 \pi^5} \sqrt{\frac{q^2 - 4m_l^2}{q^2}} \frac{1}{3q^2} \\ &\times \left[6m_l^2 |C_{10}|^2 (M_B^2 - M_K^2)^2 F_0^2(q^2) + (q^2 + 2m_l^2) \lambda(q^2) \right. \\ &\times \left| C_9^{\text{eff}} F_+(q^2) + \frac{2C_7^{\text{eff}}(m_b - m_s) F_T(q^2)}{M_B + M_K} \right|^2 \\ &\left. + |C_{10}|^2 (q^2 - 4m_l^2) \lambda(q^2) F_+^2(q^2) \right]. \end{aligned} \quad (39)$$

Our results are summarized in Table II. We have updated the prior PQCD calculations, offering more reliable and precise predictions. The q^2 -dependence branching ratio are also given in Fig.4. The two peak of branching ratio curve correspond to the possible resonance contribution such as J/Ψ and $\Psi(2S)$ in Fig.2(d). When comparing our results with those from other theoretical approaches and experimental measurements, it is evident that the theoretical predictions tend to be higher than the experimental data. This discrepancy might indicate that certain process contributions are being offset by new physics (NP) effects.

Analogous to the definition of R_K^ν , we can define

$$R_K^\ell \equiv \frac{\mathcal{B}(B \rightarrow K^+ \bar{\ell}\ell)}{\mathcal{B}(B \rightarrow K^+ \bar{\ell}\ell)|_{\text{SM}}} = 0.652 \pm 0.072, \quad (40)$$

While this discrepancy is less pronounced than that observed for R_K^ν , it nonetheless calls for a theoretical explanation.

V. LEPTOQUARKS EFFECTS

At the bottom-quark mass scale, consider the lepton flavor universality (LFU), the dimension-6 NP effective Hamiltonian of $b \rightarrow s$ semileptonic FCNC transitions can be written as [93, 114]

$$\mathcal{H}_{\text{eff}} = -\frac{4G_F}{\sqrt{2}} \frac{\alpha_{em}}{2\pi} V_{tb} V_{ts}^* \sum_{X,A,B} C_X^{AB} \mathcal{O}_X^{AB}, \quad (41)$$

with $X = V, S, T$ and $A, B = L, R$, the ten four-fermion operators

$$\begin{aligned} \mathcal{O}_V^{AB} &= (\bar{s}\gamma^\mu P_A b)(\bar{\ell}\gamma_\mu P_B \ell), \\ \mathcal{O}_S^{AB} &= (\bar{s}P_A b)(\bar{\ell}P_B \ell), \\ \mathcal{O}_T^{AB} &= \delta_{AB}(\bar{s}\sigma^{\mu\nu} P_A b)(\bar{\ell}\sigma_{\mu\nu} P_B \ell). \end{aligned} \quad (42)$$

Here, $\ell(\bar{\ell})$ donates $\nu, \ell^+(\bar{\nu}, \ell^-)$.

Considering the possible right-hand-neutrinos(RHNs) are too heavy to be produced in low-energy processes, the right-hand lepton including ℓ_R and ν_R will not be

considered in our work. Based on the previous studies [93], there are five different LQ candidates which can explaining the $B \rightarrow K$ anomaly, $S_1 = (\bar{3}, 1, 1/3)$, $\tilde{R}_2 = (3, 2, 1/6)$, $S_3 = (\bar{3}, 3, 1/3)$, $V_2 = (\bar{3}, 2, 5/6)$ and $U_3 = (3, 3, 2/3)$. Here the numbers in the brackets represent the SM gauge groups $SU(3)_C, SU(2)_L, U(1)_Y$ quantum numbers, respectively. And the former three mean the scalar LQ, the latter two stand for vector LQ. The corresponding interactions are

$$\begin{aligned} S_1 : \mathcal{L}_{S_1} &\supset +y_{1ij}^{LL} \bar{Q}_L^{C,a} S_1 \epsilon^{ab} L_L^{j,b} + \text{h.c.}, \\ \tilde{R}_2 : \mathcal{L}_{\tilde{R}_2} &\supset -\tilde{y}_{2ij}^{RL} \bar{d}_R^i \tilde{R}_2^a \epsilon^{ab} L_L^{j,b} + \text{h.c.} \\ S_3 : \mathcal{L}_{S_3} &\supset +y_{3ij}^{LL} \bar{Q}_L^{C,i,a} \epsilon^{ab} (\tau^k S_3^k)^{bc} L_L^{j,c} + \text{h.c.}, \\ V_2 : \mathcal{L}_{V_2} &\supset +x_{2ij}^{RL} \bar{d}_R^i \gamma^\mu V_{2,\mu}^a \epsilon^{ab} L_L^{j,b} + \text{h.c.} \\ U_3 : \mathcal{L}_{U_3} &\supset +x_{3ij}^{LL} \bar{Q}_L^{C,i,a} \gamma^\mu (\tau^k U_{3,\mu}^k)^{ab} L_L^{j,b} + \text{h.c.}, \end{aligned} \quad (43)$$

where we adopt the notation for LQ in Ref. [93]. After integrating out the heavy LQ field, we can obtain the corresponding wilson coefficients as shown in in Table V. Note that in order to obtain the effective coefficients in Table V, we adopt the fierz transformation into the vector current form.

Then, the general effective Hamiltonian responsible for the decay $B \rightarrow K\nu\bar{\nu}$ is written as

$$\begin{aligned} \mathcal{H}_{\text{eff}} = & -\frac{4G_F}{\sqrt{2}} \frac{\alpha_{em}}{2\pi} V_{tb} V_{ts}^* \left[C_{SM}^{LL} (\bar{s}\gamma^\mu P_L b)(\bar{\nu}\gamma_\mu P_L \nu) \right. \\ & + C_V^{LL} (\bar{s}\gamma^\mu P_L b)(\bar{\nu}\gamma_\mu P_L \nu) \\ & \left. + C_V^{RL} (\bar{s}\gamma^\mu P_R b)(\bar{\nu}\gamma_\mu P_L \nu) \right] \end{aligned} \quad (44)$$

The corresponding branching ratios are obtained by

$$\mathcal{B}(B \rightarrow K\nu\bar{\nu}) = \mathcal{B}(B \rightarrow K\nu\bar{\nu})|_{\text{SM}} \times \left| 1 + \frac{C_V^{LL} + C_V^{RL}}{C_{SM}^{LL}} \right|^2. \quad (45)$$

Therefore, the deviation between SM prediction and experimental data can be attributed to the vector current coupling LQ operator associated with the wilson coefficients $C_V^{LL,RL}$.

Comparing the experimental results and our new prediction in Eq. (31), we can obtain the viable LQ parameter ranges. As shown in Table V, the above five different types of LQ particles both can contribute to $B \rightarrow K\nu\bar{\nu}$. For simplicity, we only consider the scenario where only one type of LQ makes effect every time in the physical decay process.

Within a 1σ error range, the corresponding numerical ranges for the Wilson coefficients are estimated as

$$C_V^{LL}(S_1) = C_V^{RL}(\tilde{R}_2) = C_V^{LL}(S_3) = C_V^{RL}(V_2) = C_V^{LL}(U_3) = [-8.3, -4.5] \cup [17.1, 20.9]. \quad (46)$$

In this context, the identical coefficients across all five LQs arise from their analogous contributions to Eq. (45).

TABLE V: Tree-level Wilson coefficients of LQ models in $b \rightarrow s\nu\bar{\nu}$ and $b \rightarrow s\ell^+\ell^-$ [93], $\lambda_t = V_{tb}V_{ts}^*$, x, y are Yukawa coupling matrix elements.

	$b \rightarrow s\nu\bar{\nu}$	$b \rightarrow s\ell^+\ell^-$
$C_V^{LL}(S_1)$	$\frac{v^2}{2M_{LQ}^2} \frac{\pi}{\alpha_{em}\lambda_t} y_{1b}^{LL} y_{1s}^{LL*}$...
$C_V^{RL}(\tilde{R}_2)$	$-\frac{v^2}{2M_{LQ}^2} \frac{\pi}{\alpha_{em}\lambda_t} \tilde{y}_{2b}^{RL} \tilde{y}_{2s}^{RL*}$	$-\frac{v^2}{2M_{LQ}^2} \frac{\pi}{\alpha_{em}\lambda_t} \tilde{y}_{2b}^{RL} \tilde{y}_{2s}^{RL*}$
$C_V^{LL}(S_3)$	$\frac{v^2}{2M_{LQ}^2} \frac{\pi}{\alpha_{em}\lambda_t} y_{3b}^{LL} y_{3s}^{LL*}$	$\frac{v^2}{M_{LQ}^2} \frac{\pi}{\alpha_{em}\lambda_t} y_{3b}^{LL} y_{3s}^{LL*}$
$C_V^{RL}(V_2)$	$\frac{v^2}{M_{LQ}^2} \frac{\pi}{\alpha_{em}\lambda_t} x_{2b}^{RL} x_{2s}^{RL*}$	$\frac{v^2}{M_{LQ}^2} \frac{\pi}{\alpha_{em}\lambda_t} x_{2b}^{RL} x_{2s}^{RL*}$
$C_V^{LL}(U_3)$	$-\frac{2v^2}{M_{LQ}^2} \frac{\pi}{\alpha_{em}\lambda_t} x_{3b}^{LL} x_{3s}^{LL*}$	$-\frac{v^2}{M_{LQ}^2} \frac{\pi}{\alpha_{em}\lambda_t} x_{3b}^{LL} x_{3s}^{LL*}$

For $B^+ \rightarrow K^+\ell^+\ell^-$ process, with the addition of NP contributions, the effective Hamiltonian can be written as

$$\begin{aligned} \mathcal{H}_{\text{eff}} = & -\frac{4G_F}{\sqrt{2}} V_{tb} V_{ts}^* \frac{\alpha_{em}}{4\pi} \\ & \times \left\{ (C_{10} - C_V^{LL} - C_V^{RL}) [\bar{s}\gamma^\mu P_L b] [\bar{\ell}\gamma_\mu \gamma_5 \ell] \right. \\ & + (C_9^{\text{eff}} + C_V^{LL} + C_V^{RL}) [\bar{s}\gamma^\mu P_L b] [\bar{\ell}\gamma_\mu \ell] \\ & \left. - 2m_b C_7^{\text{eff}} \left[\bar{s}i\sigma^{\mu\nu} \frac{q_\nu}{q^2} P_R b \right] [\bar{\ell}\gamma_\mu \ell] \right\}. \end{aligned} \quad (47)$$

In this analysis, we disregard the contributions from right-handed charged leptons for simplicity. Instead, we focus solely on the leptoquarks (LQs) that contribute concurrently to both charged lepton and neutrino final states, consistent with $SU(2)_L$ gauge invariance. The corresponding Wilson coefficients are provided in Table V. Notably, S_1 does not contribute to the charged lepton process, leaving only the remaining four LQs as contributors.

With the inclusion of NP contributions, the relationship between the decay branching ratio of $B^+ \rightarrow K^+\ell^+\ell^-$ and its SM counterpart becomes more complex than suggested by Eq. (45). To address this, the differential branching ratio must be expanded based on the distinct structures of the Wilson coefficients, followed by separate integration to derive the following form as

$$\begin{aligned} \mathcal{B}(B^+ \rightarrow K^+\ell^+\ell^-) &= 0.203(6)|C_{10} - C_{10}^{\text{NP}}|^2 + 0.203(6)|C_9 + C_9^{\text{NP}}|^2 \\ &- 0.208(8)(C_9 + C_9^{\text{NP}}) + 1.063(24). \end{aligned} \quad (48)$$

Based on the above equations and Eq. (40), the corresponding numerical ranges for the coefficients $C_V^{LL,RL}$ can be determined within the 1σ uncertainty range as follows:

$$\begin{aligned} C_V^{RL}(\tilde{R}_2) &= C_V^{LL}(S_3) = C_V^{RL}(V_2) = C_V^{LL}(U_3) \\ &= [-6.96, -6.84] \cup [-0.95, -0.85]. \end{aligned} \quad (49)$$

Similar to the previous scenario, the four LQs contribute to NP in an identical manner, resulting in the same coefficient values.

These five LQ models are observed to individually account for the experimental data of the $B^+ \rightarrow K^+\nu\bar{\nu}$ and $B^+ \rightarrow K^+\ell^+\ell^-$ decay channels. By combining the results from both decay channels, the parameter space of the LQs can be further constrained. Although the Wilson coefficients for each type of LQ involved in the above two decays (charged leptons and neutrinos) differ with different factor, as presented in Table V, the underlying structure induced by Yukawa couplings and LQ masses remain consistent. Consequently, the parameter space of the LQ mass and the Yukawa coupling matrix elements, which constitute the Wilson coefficient C^{NP} , can be constrained through the FCNC $B \rightarrow K$ decays. The allowed parameter space for the five LQs is presented in Fig. 5. Additionally, the current experimental bounds on the LQ mass from colliders provide the lower limit for the masses of LQs coupled to three generations of leptons, as discussed in [8]. Considering the requirement of lepton flavor universality (LFU) in our analysis, we adopt the average lower bound of 1250 GeV for the LQ mass, as indicated in gray. For satisfying the perturbative unitarity bound, we choose the yukawa coupling $Y \leq \sqrt{4\pi}$, which leads to the product $Y_{ib}^{AB} Y_{is}^{AB*}$ across the entire range $[-4\pi, 4\pi]$

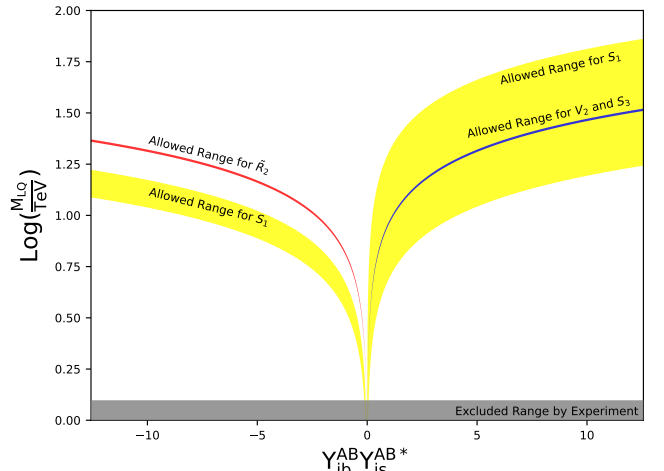


FIG. 5: The $B \rightarrow K$ decay allowed region on the LQ mass and the coupling constant ($Y = x, y$) for different LQ scenarios ($S_1, \tilde{R}_2, S_3, V_2$). The different LQ scenario is shown in different colors. The symbol A and B means the chirality (L,R). Note that the broader viable region for S_1 is due to the lack of the R_K^ℓ constraints.

As illustrated in Fig. 5, the semileptonic FCNC decay $B^+ \rightarrow K^+$ imposes significant constraints on the mass range of LQs, under the assumption that the new physics contribution arises exclusively from LQs. For the S_1 type LQ, as it does not contribute to the $B^+ \rightarrow K^+\ell^+\ell^-$ decay, its allowed parameter space is broader than those

of other LQ types. Furthermore, the product $Y_{ib}^{AB} Y_{is}^{AB*}$ spans both positive and negative values. The LQ masses exhibit opposite trends in the positive and negative coupling product ranges, increasing with positive values and decreasing with negative values. For the \tilde{R}_2 type LQs, the product of the Yukawa couplings $Y_{ib}^{AB} Y_{is}^{AB*}$ is restricted to negative values. The allowable masses of these LQs increase as the product $Y_{ib}^{AB} Y_{is}^{AB*}$ decreases. For the V_2 and S_3 type LQs, only positive values of $Y_{ib}^{AB} Y_{is}^{AB*}$ is viable and the corresponding LQ masses increase as $Y_{ib}^{AB} Y_{is}^{AB*}$ grows. Moreover, the allowed parameter spaces are consistent with each other, rendering them indistinguishable. Requiring the perturbative unitarity bound $Y_{ib}^{AB} Y_{is}^{AB*} \leq 4\pi$, we can obtain the LQ allowed upper bound 60 TeV for S_1 , 32 TeV for \tilde{R}_2 , 25 TeV for S_3 and V_2 , respectively.

Additionally, the U_3 LQ cannot reconcile the bounds from R_K^U and R_K^L as shown in Fig. 6, due to the absence of overlapping regions.

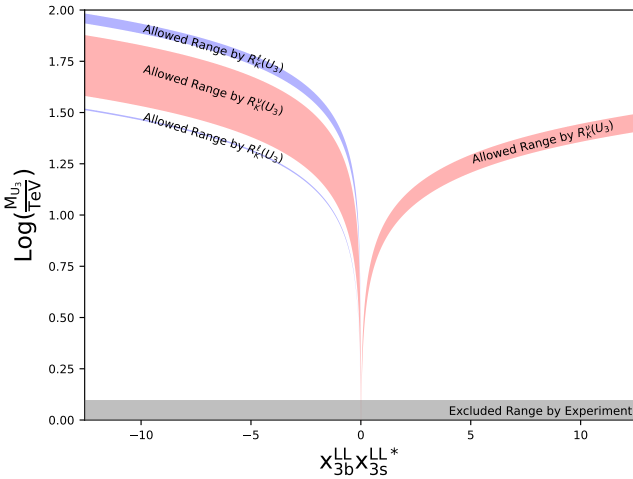


FIG. 6: The $B \rightarrow K$ decay allowed region on the LQ mass and the coupling constant for U_3 LQs scenarios. The R_K^U and R_K^L allowed region is shown in blue and red, respectively. The different LQ scenario is shown in different colors. The symbol A and B means the chirality (L,R).

VI. SUMMARY

We have analyzed the $B^+ \rightarrow K^+$ transition form factor at the next-to-leading order (NLO) and twist-3 levels within the PQCD factorization framework. Using the latest LQCD data, we conducted a comprehensive fit over the entire dynamical region, as shown in Fig. 3, thereby enhancing the reliability of the form factors. Based on these fitted form factors, we computed the branching ratio for the $B^+ \rightarrow K^+ \nu(\ell^+) \bar{\nu}(\ell^-)$ decay and provided the q^2 -dependence of the differential branching ratio in Fig. 4. This information can be directly compared with

existing experimental data. The branching ratio of these two processes are given as

$$\begin{aligned} Br(B^+ \rightarrow K^+ \nu \bar{\nu}) &= (5.70 \pm 0.17) \times 10^{-6}, \\ Br(B^+ \rightarrow K^+ \ell^+ \ell^-) &= (7.21 \pm 0.23) \times 10^{-7}. \end{aligned} \quad (50)$$

We have found that Standard Model (SM) calculations do not agree with the experimental data presented in Table II. To account for this discrepancy between our theoretical predictions and the experimental results, we explored the leptoquark (LQ) models as a potential source of new physics (NP). By incorporating five types of leptoquark models—namely S_1 , \tilde{R}_2 , S_3 , \bar{U}_1 and V_2 —we were able to explain the discrepancy and further constrain the parameter space of these leptoquarks. Constraints on the masses and Yukawa couplings of the LQs are depicted in Figs. 5. Our study indicates that leptoquarks can significantly influence the semileptonic flavor-changing neutral current $B^+ \rightarrow K^+$ decays, thereby substantially narrowing the viable parameter space for LQ masses and Yukawa couplings. We anticipate additional experimental data in the future to decrease uncertainties and enable us to rigorously test the validity of LQ models and other NP hypotheses.

ACKNOWLEDGMENTS

We thank Yi-Qi Geng for useful discussion. The work of Jin Sun is supported by IBS under the project code, IBS-R018-D1. The work of Ruilin Zhu is supported by NSFC under grant No. 12322503 and No. 12075124, and by Natural Science Foundation of Jiangsu under Grant No. BK20211267. The work of Zhi-Peng Xing is supported by NSFC under grant No.12375088, No. 12335003 and No.12405113.

Appendix A: Appendix

The NLO running coupling constant [76]

$$\alpha_s(t) = \frac{\pi}{2\beta_1 \hat{t}} - \frac{\pi \beta_2 \ln 2\hat{t}}{4\beta_1^3 \hat{t}^2}, \quad (A1)$$

with $\hat{t} = \ln(t/\Lambda)$, Λ is QCD scale, we adopt $\Lambda_{\text{QCD}} = 0.25$. The hard scales t are chosen as the maximal virtuality of the internal particles,

$$\begin{aligned} t_1 &= \max(M_B \sqrt{\eta x_2}, 1/b_1, 1/b_2), \\ t_2 &= \max(M_B \sqrt{\eta x_1}, 1/b_1, 1/b_2). \end{aligned} \quad (A2)$$

The hard functions

$$\begin{aligned} h(x_1, x_2, b_1, b_2) &= K_0(M_B \sqrt{\eta x_1 x_2} b_1) \\ &\times [\theta(b_1 - b_2) I_0(M_B \sqrt{\eta x_2} b_2) K_0(M_B \sqrt{\eta x_2} b_1) \\ &+ \theta(b_2 - b_1) I_0(M_B \sqrt{\eta x_2} b_1) K_0(M_B \sqrt{\eta x_2} b_2)]. \end{aligned} \quad (A3)$$

Sudakov exponents $S_{BP}(t) = S_B(t) + S_P(t)$

$$\begin{aligned} S_B(t) &= s\left(\frac{M_B}{\sqrt{2}}x_1, b_1\right) + \frac{5}{3} \int_{1/b_1}^t \frac{d\bar{\mu}}{\bar{\mu}} \gamma_q(\bar{\mu}), \\ S_P(t) &= s\left(\frac{M_B}{\sqrt{2}}x_2, b_2\right) + s\left(\frac{M_B}{\sqrt{2}}(1-x_2), b_2\right) \\ &\quad + 2 \int_{1/b_2}^t \frac{d\bar{\mu}}{\bar{\mu}} \gamma_q(\bar{\mu}), \end{aligned} \quad (\text{A4})$$

where $\gamma_q = -\alpha_s/\pi$ is the quark anomalous dimension, the expression for $s(Q, b)$ can be written as [76]

$$\begin{aligned} s(Q, b) &= \frac{A^{(1)}}{2\beta_1} \hat{q} \ln\left(\frac{\hat{q}}{\hat{b}}\right) + \frac{A^{(2)}}{4\beta_1^2} \left(\frac{\hat{q}}{\hat{b}} - 1\right) - \frac{A^{(1)}}{2\beta_1} \left(\hat{q} - \hat{b}\right) \\ &\quad - \frac{A^{(1)}\beta_2}{4\beta_1^3} \hat{q} \left[\frac{\ln(2\hat{b}) + 1}{\hat{b}} - \frac{\ln(2\hat{q}) + 1}{\hat{q}} \right] \\ &\quad - \left[\frac{A^{(2)}}{4\beta_1^2} - \frac{A^{(1)}}{4\beta_1} \ln\left(\frac{e^{2\gamma-1}}{2}\right) \right] \ln\left(\frac{\hat{q}}{\hat{b}}\right) \\ &\quad + \frac{A^{(1)}\beta_2}{8\beta_1^3} \left[\ln^2(2\hat{q}) - \ln^2(2\hat{b}) \right], \end{aligned} \quad (\text{A5})$$

where

$$\begin{aligned} \hat{q} &= \ln\left[Q/(\sqrt{2}\Lambda)\right], \quad \hat{b} = \ln\left(1/(b\Lambda)\right), \\ \beta_1 &= \frac{33-2n_f}{12}, \quad \beta_2 = \frac{153-19n_f}{24}, \\ A^{(1)} &= \frac{4}{3}, \quad A^{(2)} = \frac{67}{9} - \frac{\pi^2}{3} - \frac{10n_f}{27} + \frac{8}{3}\beta_1 \ln\left(\frac{e^\gamma}{2}\right). \end{aligned} \quad (\text{A6})$$

Threshold resummation factor [77]

$$S_t(x) = \frac{2^{1+2c}\Gamma(3/2+c)}{\sqrt{\pi}\Gamma(1+c)} [x(1-x)]^c, \quad (\text{A7})$$

with $c = 0.3$.

NLO hard kernel correction factor at twist-2 [106]

$$\begin{aligned} F_{\text{T2}}^{(1)}(x_i, \mu, t, q^2) &= \frac{\alpha_s(t)C_F}{4\pi} \left[\frac{21}{4} \ln \frac{\mu^2}{M_B^2} \right. \\ &\quad - \left(\ln \frac{M_B^2}{\xi_1^2} + \frac{13}{2} \right) \ln \frac{t^2}{M_B^2} + \frac{7}{16} \ln^2(x_1 x_2) + \frac{1}{8} \ln^2 x_1 \\ &\quad + \frac{1}{4} \ln x_1 \ln x_2 + \left(2 \ln \frac{M_B^2}{\xi_1^2} + \frac{7}{8} \ln \eta - \frac{1}{4} \right) \ln x_1 \\ &\quad + \left(\frac{7}{8} \ln \eta - \frac{3}{2} \right) \ln x_2 + \left(\frac{15}{4} - \frac{7}{16} \ln \eta \right) \ln \eta \\ &\quad \left. - \frac{1}{2} \ln \frac{M_B^2}{\xi_1^2} \left(3 \ln \frac{M_B^2}{\xi_1^2} + 2 \right) + \frac{101\pi^2}{48} + \frac{219}{16} \right], \end{aligned} \quad (\text{A8})$$

with

$$\mu = \left\{ \exp \left[c_1 + \left(\ln \frac{M_B^2}{\xi_1^2} + \frac{5}{4} \right) \ln \frac{t^2}{M_B^2} \right] x_1^{c_2} x_2^{c_3} \right\}^{2/21} \cdot t, \quad (\text{A9})$$

with

$$\begin{aligned} c_1 &= - \left(\frac{15}{4} - \frac{7}{16} \ln \eta \right) \ln \eta + \frac{1}{2} \ln \frac{M_B^2}{\xi_1^2} \left(3 \ln \frac{M_B^2}{\xi_1^2} + 2 \right) \\ &\quad - \frac{101\pi^2}{48} - \frac{219}{16}, \\ c_2 &= - \left(2 \ln \frac{M_B^2}{\xi_1^2} + \frac{7}{8} \ln \eta - \frac{1}{4} \right), \\ c_3 &= - \frac{7}{8} \ln \eta + \frac{3}{2}. \end{aligned} \quad (\text{A10})$$

NLO hard kernel correction factor at twist-3 [107]

$$\begin{aligned} F_{\text{T3}}^{(1)}(x_i, \mu, t, q^2) &= \frac{\alpha_s(t)C_F}{4\pi} \left[\frac{21}{4} \ln \frac{\mu^2}{M_B^2} \right. \\ &\quad - \frac{1}{2} (6 + \ln \frac{M_B^2}{\xi_1^2}) \ln \frac{t^2}{M_B^2} + \frac{7}{16} \ln^2 x_1 - \frac{3}{8} \ln^2 x_2 \\ &\quad + \frac{9}{8} \ln x_1 \ln x_2 + \left(-\frac{29}{8} + \ln \frac{M_B^2}{\xi_1^2} + \frac{15}{8} \ln \eta \right) \ln x_1 \\ &\quad + \left(-\frac{25}{16} + \ln \frac{M_B^2}{\xi_2^2} + \frac{9}{8} \ln \eta \right) \ln x_2 + \frac{1}{2} \ln \frac{M_B^2}{\xi_1^2} \\ &\quad \left. - \frac{1}{4} \ln^2 \frac{M_B^2}{\xi_1^2} + \ln \frac{M_B^2}{\xi_2^2} - \frac{9}{8} \ln \eta - \frac{1}{8} \ln^2 \eta + \frac{37\pi^2}{32} + \frac{91}{32} \right], \end{aligned} \quad (\text{A11})$$

with

$$\mu = \left\{ \exp \left[c_1 + \left(\frac{1}{2} \ln \frac{M_B^2}{\xi_1^2} - \frac{9}{4} \right) \ln \frac{t^2}{M_B^2} \right] x_1^{c_2} x_2^{c_3} \right\}^{2/21} \cdot t, \quad (\text{A12})$$

with

$$\begin{aligned} c_1 &= - \left(\frac{1}{2} - \frac{1}{4} \ln \frac{M_B^2}{\xi_1^2} \right) \ln \frac{M_B^2}{\xi_1^2} + \left(\frac{9}{8} + \frac{1}{8} \ln \eta \right) \ln \eta \\ &\quad - \frac{379}{32} - \frac{167\pi^2}{96}, \\ c_2 &= \frac{29}{8} - \ln \frac{M_B^2}{\xi_1^2} - \frac{15}{8} \ln \eta, \\ c_3 &= \frac{25}{16} - \frac{9}{8} \ln \eta, \end{aligned} \quad (\text{A13})$$

where $\xi_1 = 25M_B$, $\xi_2^2 = M_B^2$.

-
- [1] V. Khachatryan *et al.* [CMS and LHCb], Nature **522**, 68-72 (2015) doi:10.1038/nature14474 [arXiv:1411.4413 [hep-ex]].
- [2] R. Aaij *et al.* [LHCb], Phys. Rev. Lett. **113**, 151601 (2014) doi:10.1103/PhysRevLett.113.151601 [arXiv:1406.6482 [hep-ex]].
- [3] S. Wehle *et al.* [Belle], Phys. Rev. Lett. **118**, no.11, 111801 (2017) doi:10.1103/PhysRevLett.118.111801 [arXiv:1612.05014 [hep-ex]].
- [4] R. Aaij *et al.* [LHCb], JHEP **08**, 055 (2017) doi:10.1007/JHEP08(2017)055 [arXiv:1705.05802 [hep-ex]].
- [5] J. Grygier *et al.* [Belle], Phys. Rev. D **96**, no.9, 091101 (2017) doi:10.1103/PhysRevD.96.091101 [arXiv:1702.03224 [hep-ex]].
- [6] R. Aaij *et al.* [LHCb], Phys. Rev. Lett. **125**, no.1, 011802 (2020) doi:10.1103/PhysRevLett.125.011802 [arXiv:2003.04831 [hep-ex]].
- [7] R. Aaij *et al.* [LHCb], Nature Phys. **18**, no.3, 277-282 (2022) doi:10.1038/s41567-023-02095-3 [arXiv:2103.11769 [hep-ex]].
- [8] S. Navas *et al.* [Particle Data Group], Phys. Rev. D **110**, no.3, 030001 (2024) doi:10.1103/PhysRevD.110.030001
- [9] I. Adachi *et al.* [Belle-II], Phys. Rev. D **109**, no.11, 112006 (2024) doi:10.1103/PhysRevD.109.112006 [arXiv:2311.14647 [hep-ex]].
- [10] H. J. Tian, H. B. Fu, T. Zhong, Y. X. Wang and X. G. Wu, [arXiv:2411.12141 [hep-ph]].
- [11] W. Altmannshofer and S. Roy, [arXiv:2411.06592 [hep-ph]].
- [12] D. Bećirević, S. Fajfer, N. Košnik and L. Pavičić, [arXiv:2410.23257 [hep-ph]].
- [13] L. Allwicher, M. Bordone, G. Isidori, G. Piazza and A. Stanzione, [arXiv:2410.21444 [hep-ph]].
- [14] K. Dash, P. C. Dash, R. N. Panda, S. Kar and N. Barik, Phys. Rev. D **110**, no.11, 113010 (2024) doi:10.1103/PhysRevD.110.113010 [arXiv:2410.06951 [hep-ph]].
- [15] Z. S. Wang, Y. Zhang and W. Liu, [arXiv:2410.00491 [hep-ph]].
- [16] C. Hati, J. Leite, N. Nath and J. W. F. Valle, [arXiv:2408.00060 [hep-ph]].
- [17] O. Sumensari, [arXiv:2406.00218 [hep-ph]].
- [18] C. S. Kim, D. Sahoo and K. N. Vishnudath, Eur. Phys. J. C **84**, no.9, 882 (2024) doi:10.1140/epjc/s10052-024-13262-y [arXiv:2405.17341 [hep-ph]].
- [19] M. Andersson, A. M. Marshall, K. A. Petridis and E. Smith, Symmetry **16**, no.6, 638 (2024) doi:10.3390/sym16060638
- [20] A. J. Buras, J. Harz and M. A. Mojahed, JHEP **10**, 087 (2024) doi:10.1007/JHEP10(2024)087 [arXiv:2405.06742 [hep-ph]].
- [21] S. Rosauro-Alcaraz and L. P. S. Leal, Eur. Phys. J. C **84**, no.8, 795 (2024) doi:10.1140/epjc/s10052-024-13104-x [arXiv:2404.17440 [hep-ph]].
- [22] S. Karmakar, A. Dighe and R. S. Gupta, [arXiv:2404.10061 [hep-ph]].
- [23] D. Marzocca, M. Nardecchia, A. Stanzione and C. Toni, Eur. Phys. J. C **84**, no.11, 1217 (2024) doi:10.1140/epjc/s10052-024-13534-7 [arXiv:2404.06533 [hep-ph]].
- [24] P. D. Bolton, S. Fajfer, J. F. Kamenik and M. Novoa-Brunet, Phys. Rev. D **110**, no.5, 055001 (2024) doi:10.1103/PhysRevD.110.055001 [arXiv:2403.13887 [hep-ph]].
- [25] X. G. He, X. D. Ma, M. A. Schmidt, G. Valencia and R. R. Volkas, JHEP **07**, 168 (2024) doi:10.1007/JHEP07(2024)168 [arXiv:2403.12485 [hep-ph]].
- [26] C. H. Chen and C. W. Chiang, Phys. Rev. D **110**, no.7, 075036 (2024) doi:10.1103/PhysRevD.110.075036 [arXiv:2403.02897 [hep-ph]].
- [27] B. F. Hou, X. Q. Li, M. Shen, Y. D. Yang and X. B. Yuan, JHEP **06**, 172 (2024) doi:10.1007/JHEP06(2024)172 [arXiv:2402.19208 [hep-ph]].
- [28] T. Li, Z. Qian, M. A. Schmidt and M. Yuan, JHEP **05**, 232 (2024) doi:10.1007/JHEP05(2024)232 [arXiv:2402.14232 [hep-ph]].
- [29] E. Gabrielli, L. Marzola, K. Müürsepp and M. Raidal, Eur. Phys. J. C **84**, no.5, 460 (2024) doi:10.1140/epjc/s10052-024-12818-2 [arXiv:2402.05901 [hep-ph]].
- [30] F. Loparco, Particles **7**, no.1, 161-178 (2024) doi:10.3390/particles7010009 [arXiv:2401.11999 [hep-ph]].
- [31] F. Z. Chen, Q. Wen and F. Xu, Eur. Phys. J. C **84**, no.10, 1012 (2024) doi:10.1140/epjc/s10052-024-13425-x [arXiv:2401.11552 [hep-ph]].
- [32] S. Y. Ho, J. Kim and P. Ko, [arXiv:2401.10112 [hep-ph]].
- [33] K. Fridell, M. Ghosh, T. Okui and K. Tobioka, Phys. Rev. D **109**, no.11, 11 (2024) doi:10.1103/PhysRevD.109.115006 [arXiv:2312.12507 [hep-ph]].
- [34] D. McKeen, J. N. Ng and D. Tuckler, Phys. Rev. D **109**, no.7, 075006 (2024) doi:10.1103/PhysRevD.109.075006 [arXiv:2312.00982 [hep-ph]].
- [35] W. Altmannshofer, A. Crivellin, H. Haigh, G. Inguglia and J. Martin Camalich, Phys. Rev. D **109**, no.7, 075008 (2024) doi:10.1103/PhysRevD.109.075008 [arXiv:2311.14629 [hep-ph]].
- [36] A. Datta, D. Marfatia and L. Mukherjee, Phys. Rev. D **109**, no.3, L031701 (2024) doi:10.1103/PhysRevD.109.L031701 [arXiv:2310.15136 [hep-ph]].
- [37] A. Berezhnoy and D. Melikhov, EPL **145**, no.1, 14001 (2024) doi:10.1209/0295-5075/ad1d03 [arXiv:2309.17191 [hep-ph]].
- [38] X. G. He, X. D. Ma and G. Valencia, Phys. Rev. D **109**, no.7, 075019 (2024) doi:10.1103/PhysRevD.109.075019 [arXiv:2309.12741 [hep-ph]].
- [39] Y. Amhis, M. Kenzie, M. Reboud and A. R. Wiederhold, JHEP **01**, 144 (2024) doi:10.1007/JHEP01(2024)144 [arXiv:2309.11353 [hep-ex]].
- [40] M. Abdughani and Y. Reyimuaaji, Phys. Rev. D **110**, no.5, 055013 (2024) doi:10.1103/PhysRevD.110.055013 [arXiv:2309.03706 [hep-ph]].
- [41] L. Allwicher, D. Bećirević, G. Piazza, S. Rosauro-Alcaraz and O. Sumensari, Phys. Lett. B **848**, 138411 (2024) doi:10.1016/j.physletb.2023.138411 [arXiv:2309.02246 [hep-ph]].

- [42] R. Bause, H. Gisbert and G. Hiller, Phys. Rev. D **109**, no.1, 015006 (2024) doi:10.1103/PhysRevD.109.015006 [arXiv:2309.00075 [hep-ph]].
- [43] P. Athron, R. Martinez and C. Sierra, JHEP **02**, 121 (2024) doi:10.1007/JHEP02(2024)121 [arXiv:2308.13426 [hep-ph]].
- [44] Z. J. Xiao and X. Liu, Chin. Sci. Bull. **59**, 3748-3759 (2014) doi:10.1007/s11434-014-0418-z [arXiv:1401.0151 [hep-ph]].
- [45] H. s. Wang, S. m. Liu, J. Cao, X. Liu and Z. j. Xiao, Nucl. Phys. A **930**, 117-130 (2014) doi:10.1016/j.nuclphysa.2014.08.001
- [46] X. Liu, Z. J. Xiao and Z. T. Zou, Phys. Rev. D **94**, no.11, 113005 (2016) doi:10.1103/PhysRevD.94.113005 [arXiv:1609.01024 [hep-ph]].
- [47] X. Liu, R. H. Li, Z. T. Zou and Z. J. Xiao, Phys. Rev. D **96**, no.1, 013005 (2017) doi:10.1103/PhysRevD.96.013005 [arXiv:1703.05982 [hep-ph]].
- [48] H. s. Wang, X. l. Wang, F. n. Zheng, S. m. Liu, J. Cao and Q. s. Wang, Nucl. Phys. B **919**, 25-40 (2017) doi:10.1016/j.nuclphysb.2017.03.008
- [49] C. D. Lü, Y. L. Shen, Y. M. Wang and Y. B. Wei, JHEP **01**, 024 (2019) doi:10.1007/JHEP01(2019)024 [arXiv:1810.00819 [hep-ph]].
- [50] J. Hua, Y. L. Zhang and Z. J. Xiao, Phys. Rev. D **99**, no.1, 016007 (2019) doi:10.1103/PhysRevD.99.016007 [arXiv:1810.08738 [hep-ph]].
- [51] Y. L. Shen, Z. T. Zou and Y. B. Wei, Phys. Rev. D **99**, no.1, 016004 (2019) doi:10.1103/PhysRevD.99.016004 [arXiv:1811.08250 [hep-ph]].
- [52] L. Su, Z. Jiang and X. Liu, J. Phys. G **46**, no.8, 085003 (2019) doi:10.1088/1361-6471/ab2814 [arXiv:1906.04438 [hep-ph]].
- [53] S. Cheng and Z. J. Xiao, Front. Phys. (Beijing) **16**, no.2, 24201 (2021) doi:10.1007/s11467-020-1036-7 [arXiv:2009.02872 [hep-ph]].
- [54] S. P. Jin, X. Q. Hu and Z. J. Xiao, Phys. Rev. D **102**, no.1, 013001 (2020) doi:10.1103/PhysRevD.102.013001 [arXiv:2003.12226 [hep-ph]].
- [55] J. Hua, H. n. Li, C. D. Lu, W. Wang and Z. P. Xing, Phys. Rev. D **104**, no.1, 016025 (2021) doi:10.1103/PhysRevD.104.016025 [arXiv:2012.15074 [hep-ph]].
- [56] J. Chai, S. Cheng, Y. h. Ju, D. C. Yan, C. D. Lü and Z. J. Xiao, Chin. Phys. C **46**, no.12, 123103 (2022) doi:10.1088/1674-1137/ac88bd [arXiv:2207.04190 [hep-ph]].
- [57] X. Liu, Phys. Rev. D **108**, no.9, 096006 (2023) doi:10.1103/PhysRevD.108.096006 [arXiv:2305.00713 [hep-ph]].
- [58] R. X. Wang and M. Z. Yang, [arXiv:2411.08454 [hep-ph]].
- [59] C. Bouchard *et al.* [HPQCD], Phys. Rev. D **88**, no.5, 054509 (2013) [erratum: Phys. Rev. D **88**, no.7, 079901 (2013)] doi:10.1103/PhysRevD.88.054509 [arXiv:1306.2384 [hep-lat]].
- [60] C. Bouchard *et al.* [HPQCD], Phys. Rev. Lett. **111**, no.16, 162002 (2013) [erratum: Phys. Rev. Lett. **112**, no.14, 149902 (2014)] doi:10.1103/PhysRevLett.111.162002 [arXiv:1306.0434 [hep-ph]].
- [61] C. M. Bouchard, G. P. Lepage, C. Monahan, H. Na and J. Shigemitsu, Phys. Rev. D **90**, 054506 (2014) doi:10.1103/PhysRevD.90.054506 [arXiv:1406.2279 [hep-lat]].
- [62] J. M. Flynn, T. Izubuchi, T. Kawanai, C. Lehner, A. Soni, R. S. Van de Water and O. Witzel, Phys. Rev. D **91**, no.7, 074510 (2015) doi:10.1103/PhysRevD.91.074510 [arXiv:1501.05373 [hep-lat]].
- [63] J. A. Bailey, A. Bazavov, C. Bernard, C. M. Bouchard, C. DeTar, D. Du, A. X. El-Khadra, J. Foley, E. D. Freeland and E. Gámiz, *et al.* Phys. Rev. D **93**, no.2, 025026 (2016) doi:10.1103/PhysRevD.93.025026 [arXiv:1509.06235 [hep-lat]].
- [64] J. A. Bailey *et al.* [Fermilab Lattice and MILC], Phys. Rev. D **92**, no.1, 014024 (2015) doi:10.1103/PhysRevD.92.014024 [arXiv:1503.07839 [hep-lat]].
- [65] A. Bazavov *et al.* [Fermilab Lattice and MILC], Phys. Rev. D **100**, no.3, 034501 (2019) doi:10.1103/PhysRevD.100.034501 [arXiv:1901.02561 [hep-lat]].
- [66] B. Colquhoun *et al.* [JLQCD], Phys. Rev. D **106**, no.5, 054502 (2022) doi:10.1103/PhysRevD.106.054502 [arXiv:2203.04938 [hep-lat]].
- [67] G. Martinelli, S. Simula and L. Vittorio, JHEP **08**, 022 (2022) doi:10.1007/JHEP08(2022)022 [arXiv:2202.10285 [hep-ph]].
- [68] J. M. Flynn *et al.* [RBC/UKQCD], Phys. Rev. D **107**, no.11, 114512 (2023) doi:10.1103/PhysRevD.107.114512 [arXiv:2303.11280 [hep-lat]].
- [69] Y. M. Wang and Y. L. Shen, Nucl. Phys. B **898**, 563-604 (2015) doi:10.1016/j.nuclphysb.2015.07.016 [arXiv:1506.00667 [hep-ph]].
- [70] Y. L. Shen, Y. B. Wei and C. D. Lü, Phys. Rev. D **97**, no.5, 054004 (2018) doi:10.1103/PhysRevD.97.054004 [arXiv:1607.08727 [hep-ph]].
- [71] A. V. Rusov, Eur. Phys. J. C **77**, no.7, 442 (2017) doi:10.1140/epjc/s10052-017-5000-9 [arXiv:1705.01929 [hep-ph]].
- [72] N. Gubernari, A. Kokulu and D. van Dyk, JHEP **01**, 150 (2019) doi:10.1007/JHEP01(2019)150 [arXiv:1811.00983 [hep-ph]].
- [73] R. Y. Zhou, L. Guo, H. B. Fu, W. Cheng and X. G. Wu, Chin. Phys. C **44**, no.1, 013101 (2020) doi:10.1088/1674-1137/44/1/013101 [arXiv:1910.10965 [hep-ph]].
- [74] Y. L. Shen and Y. B. Wei, Adv. High Energy Phys. **2022**, 2755821 (2022) doi:10.1155/2022/2755821 [arXiv:2112.01500 [hep-ph]].
- [75] H. n. Li and G. F. Sterman, Nucl. Phys. B **381**, 129-140 (1992) doi:10.1016/0550-3213(92)90643-P
- [76] H. n. Li and H. L. Yu, Phys. Rev. D **53**, 2480-2490 (1996) doi:10.1103/PhysRevD.53.2480 [arXiv:hep-ph/9411308 [hep-ph]].
- [77] T. Kurimoto, H. n. Li and A. I. Sanda, Phys. Rev. D **65**, 014007 (2002) doi:10.1103/PhysRevD.65.014007 [arXiv:hep-ph/0105003 [hep-ph]].
- [78] H. n. Li, Prog. Part. Nucl. Phys. **51**, 85-171 (2003) doi:10.1016/S0146-6410(03)90013-5 [arXiv:hep-ph/0303116 [hep-ph]].
- [79] Y. Li, C. D. Lu, Z. J. Xiao and X. Q. Yu, Phys. Rev. D **70**, 034009 (2004) doi:10.1103/PhysRevD.70.034009 [arXiv:hep-ph/0404028 [hep-ph]].
- [80] A. Ali, G. Kramer, Y. Li, C. D. Lu, Y. L. Shen,

- W. Wang and Y. M. Wang, Phys. Rev. D **76**, 074018 (2007) doi:10.1103/PhysRevD.76.074018 [arXiv:hep-ph/0703162 [hep-ph]].
- [81] Z. J. Xiao, W. F. Wang and Y. y. Fan, Phys. Rev. D **85**, 094003 (2012) doi:10.1103/PhysRevD.85.094003 [arXiv:1111.6264 [hep-ph]].
- [82] J. J. Qi, Z. Y. Wang, X. H. Guo, X. W. Kang and Z. H. Zhang, Nucl. Phys. B **948**, 114788 (2019) doi:10.1016/j.nuclphysb.2019.114788 [arXiv:1811.10333 [hep-ph]].
- [83] W. G. Parrott *et al.* [(HPQCD collaboration)§ and HPQCD], Phys. Rev. D **107**, no.1, 014510 (2023) doi:10.1103/PhysRevD.107.014510 [arXiv:2207.12468 [hep-lat]].
- [84] W. F. Wang and Z. J. Xiao, Phys. Rev. D **86**, 114025 (2012) doi:10.1103/PhysRevD.86.114025 [arXiv:1207.0265 [hep-ph]].
- [85] J. C. Pati and A. Salam, Phys. Rev. D **8**, 1240-1251 (1973) doi:10.1103/PhysRevD.8.1240
- [86] J. C. Pati and A. Salam, Phys. Rev. D **10**, 275-289 (1974) [erratum: Phys. Rev. D **11**, 703-703 (1975)] doi:10.1103/PhysRevD.10.275
- [87] M. Bauer and M. Neubert, Phys. Rev. Lett. **116**, no.14, 141802 (2016) doi:10.1103/PhysRevLett.116.141802 [arXiv:1511.01900 [hep-ph]].
- [88] D. Bećirević, I. Doršner, S. Fajfer, N. Košnik, D. A. Faroughy and O. Sumensari, Phys. Rev. D **98**, no.5, 055003 (2018) doi:10.1103/PhysRevD.98.055003 [arXiv:1806.05689 [hep-ph]].
- [89] S. Fajfer and N. Košnik, Phys. Lett. B **755**, 270-274 (2016) doi:10.1016/j.physletb.2016.02.018 [arXiv:1511.06024 [hep-ph]].
- [90] D. Bećirević, S. Fajfer, N. Košnik and L. Pavičić, Phys. Rev. D **110**, no.5, 5 (2024) doi:10.1103/PhysRevD.110.055023 [arXiv:2404.16772 [hep-ph]].
- [91] C. H. Chen and C. W. Chiang, Phys. Rev. D **109**, no.7, 075004 (2024) doi:10.1103/PhysRevD.109.075004 [arXiv:2309.12904 [hep-ph]].
- [92] W. Buchmuller, R. Ruckl and D. Wyler, Phys. Lett. B **191**, 442-448 (1987) [erratum: Phys. Lett. B **448**, 320-320 (1999)] doi:10.1016/0370-2693(87)90637-X
- [93] I. Doršner, S. Fajfer, A. Greljo, J. F. Kamenik and N. Košnik, Phys. Rept. **641**, 1-68 (2016) doi:10.1016/j.physrep.2016.06.001 [arXiv:1603.04993 [hep-ph]].
- [94] A. Szczepaniak, E. M. Henley and S. J. Brodsky, Phys. Lett. B **243**, 287-292 (1990) doi:10.1016/0370-2693(90)90853-X
- [95] G. Burdman and J. F. Donoghue, Phys. Lett. B **270**, 55-60 (1991) doi:10.1016/0370-2693(91)91538-7
- [96] M. Beneke and T. Feldmann, Nucl. Phys. B **592**, 3-34 (2001) doi:10.1016/S0550-3213(00)00585-X [arXiv:hep-ph/0008255 [hep-ph]].
- [97] J. P. Ralston and P. Jain, Phys. Rev. D **69**, 053008 (2004) doi:10.1103/PhysRevD.69.053008 [arXiv:hep-ph/0302043 [hep-ph]].
- [98] H. n. Li and H. L. Yu, Phys. Rev. Lett. **74**, 4388-4391 (1995) doi:10.1103/PhysRevLett.74.4388 [arXiv:hep-ph/9409313 [hep-ph]].
- [99] P. Ball and R. Zwicky, Phys. Rev. D **71**, 014015 (2005) doi:10.1103/PhysRevD.71.014015 [arXiv:hep-ph/0406232 [hep-ph]].
- [100] P. Ball, V. M. Braun and A. Lenz, JHEP **05**, 004 (2006) doi:10.1088/1126-6708/2006/05/004 [arXiv:hep-ph/0603063 [hep-ph]].
- [101] P. Ball and G. W. Jones, JHEP **03**, 069 (2007) doi:10.1088/1126-6708/2007/03/069 [arXiv:hep-ph/0702100 [hep-ph]].
- [102] G. S. Bali *et al.* [RQCD], Phys. Lett. B **774**, 91-97 (2017) doi:10.1016/j.physletb.2017.08.077 [arXiv:1705.10236 [hep-lat]].
- [103] G. S. Bali *et al.* [RQCD], JHEP **08**, 065 (2019) doi:10.1007/JHEP08(2019)065 [arXiv:1903.08038 [hep-lat]].
- [104] J. Hua *et al.* [Lattice Parton], Phys. Rev. Lett. **127**, no.6, 062002 (2021) doi:10.1103/PhysRevLett.127.062002 [arXiv:2011.09788 [hep-lat]].
- [105] G. Buchalla, A. J. Buras and M. E. Lautenbacher, Rev. Mod. Phys. **68**, 1125-1144 (1996) doi:10.1103/RevModPhys.68.1125 [arXiv:hep-ph/9512380 [hep-ph]].
- [106] H. n. Li, Y. L. Shen and Y. M. Wang, Phys. Rev. D **85**, 074004 (2012) doi:10.1103/PhysRevD.85.074004 [arXiv:1201.5066 [hep-ph]].
- [107] S. Cheng, Y. Y. Fan, X. Yu, C. D. Lü and Z. J. Xiao, Phys. Rev. D **89**, no.9, 094004 (2014) doi:10.1103/PhysRevD.89.094004 [arXiv:1402.5501 [hep-ph]].
- [108] T. Blake, G. Lanfranchi and D. M. Straub, Prog. Part. Nucl. Phys. **92**, 50-91 (2017) doi:10.1016/j.ppnp.2016.10.001 [arXiv:1606.00916 [hep-ph]].
- [109] A. J. Buras, J. Girrbach-Noe, C. Niehoff and D. M. Straub, JHEP **02**, 184 (2015) doi:10.1007/JHEP02(2015)184 [arXiv:1409.4557 [hep-ph]].
- [110] W. G. Parrott *et al.* [HPQCD], Phys. Rev. D **107**, no.1, 014511 (2023) [erratum: Phys. Rev. D **107**, no.11, 119903 (2023)] doi:10.1103/PhysRevD.107.014511 [arXiv:2207.13371 [hep-ph]].
- [111] B. Y. Cui, Y. K. Huang, Y. L. Shen, C. Wang and Y. M. Wang, JHEP **03**, 140 (2023) doi:10.1007/JHEP03(2023)140 [arXiv:2212.11624 [hep-ph]].
- [112] C. Bourrely, I. Caprini and L. Lellouch, Phys. Rev. D **79**, 013008 (2009) [erratum: Phys. Rev. D **82**, 099902 (2010)] doi:10.1103/PhysRevD.82.099902 [arXiv:0807.2722 [hep-ph]].
- [113] J. F. Kamenik and C. Smith, Phys. Lett. B **680**, 471-475 (2009) doi:10.1016/j.physletb.2009.09.041 [arXiv:0908.1174 [hep-ph]].
- [114] T. E. Browder, N. G. Deshpande, R. Mandal and R. Sinha, Phys. Rev. D **104**, no.5, 053007 (2021) doi:10.1103/PhysRevD.104.053007 [arXiv:2107.01080 [hep-ph]].